THE JOURNAL OF PHYSICAL CHEMISTRY B

ARTICLE

pubs.acs.org/JPCB

Maxwell−Stefan Diffusivities in Binary Mixtures of Ionic Liquids with Dimethyl Sulfoxide (DMSO) and H_2O

Xin Liu,[†,‡] Thijs J. H. Vlugt,[‡] and André Bardow*[,†,‡]

[†]Lehrstuhl für Technische Thermodynamik, RWTH Aachen University, Schinkelstrasse 8, 52062 Aachen, Germany

[‡]Process & Energy Laboratory, Delft University of Technology, Leeghwaterstraat 44, 2628 CA Delft, The Netherlands

Supporting Information

ABSTRACT: Ionic liquids (ILs) are promising solvents for applications ranging from CO_2 capture to the pretreatment of biomass. However, slow diffusion often restricts their applicability. A thorough understanding of diffusion in ILs is therefore highly desirable. Previous research largely focused on self-diffusion in ILs. For practical applications, mutual diffusion is by far more important than self-diffusion. For describing mutual diffusion in multicomponent systems, the Maxwell−Stefan (MS) approach is commonly used. Unfortunately, it is difficult to obtain MS diffusivities from experiments, but they can be directly extracted from molecular dynamics (MD) simulations. In this work, MS diffusivities were computed in binary systems containing 1-alkyl-3-methylimidazolium chloride ($C_n$mimCl, n = 2, 4, 8), water, and/or dimethyl sulfoxide (DMSO) using MD. The dependence of self- and MS diffusivities on mixture composition was investigated. Our results show the following: (1) For solutions of ILs in water and DMSO, self-diffusivities decrease strongly with increasing IL concentration. For DMSO-IL, a single exponential decay is observed. (2) In both water−IL and DMSO−IL, MS diffusivities vary by a factor of 10 within the concentration range which is, however, still significantly smaller than the variation of the self-diffusion coefficients. (3) The MS diffusivities of the IL are almost independent of the alkyl chain length. (4) ILs stay in a form of isolated ions in $C_n$mimCl−H_2O mixtures; however, dissociation into ions is much less observed in $C_n$mimCl−DMSO systems. This has a large effect on the concentration dependence of MS diffusivities. (5) Recently, we proposed a new model for predicting the MS diffusivity at infinite dilution, that is, $Đ_{ij}^{x_k \to 1}$ (*Ind. Eng. Chem. Res.* **2011**, *50*, 4776−4782). This quantity describes the friction between components i and j when both are infinitely diluted in component k. In contrast to earlier empirical models, our model is based on the linear response theory and the Onsager relations which allows a clear interpretation of the results. The key assumption in the model is that velocity cross-correlations are neglected. The present study clearly shows that velocity cross-correlation functions in ILs cannot be neglected and that the dissociation of ILs into ions has a very strong influence on diffusion.

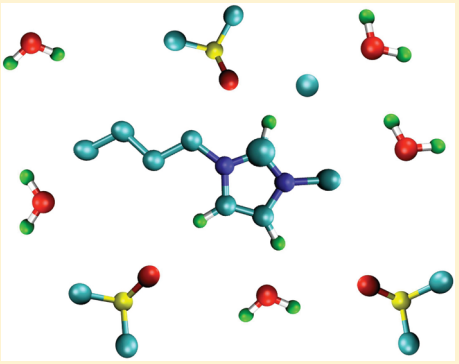

1. INTRODUCTION

Ionic liquids (ILs) are salts which have melting points below 100 °C. An enormous number of different ILs can be prepared by a well-chosen selection of the cation and anion pair.[1,2] They offer an alternative to common organic solvents.[3−5] Several properties make ILs popular, like small vapor pressure, thermal stability, and the ability to dissolve a wide range of compounds.[6,7] Imidazolium-based ILs as shown in Figure 1 are widely studied in both experiments and computer simulations as these ILs are already used in practice and are easy to synthesize.[1,2,7−9]

The study of diffusion in ILs receives increasing interest as diffusion restricts the applicability of ILs in many processes. Self-diffusion of these systems was extensively studied in the past. This quantity can be measured using pulsed-field gradient nuclear magnetic resonance (PFG-NMR) spectroscopy. For instance, Lovell et al. studied the dependence of self-diffusivities on concentration in 1-ethyl-3-methylimidazolium acetate cellulose.[10] Iacob et al. measured self-diffusivities of 1-hexyl-3-methylimidazolium hexafluorophosphate in silica membranes.[11] Bara et al. studied self-diffusivities of flue gases absorbed in imidazolium-based ILs and provided guidelines for separating CO_2 from flue gases using imidazolium-based ILs.[12] To gain a molecular understanding of diffusion, molecular dynamics (MD) simulations are often used. However, the nature of ILs implies strong electrostatic interactions which significantly increases the computational cost for obtaining adequate sampling.[13] This becomes even more severe for computing collective properties like transport diffusivities.[14,15] While previous studies on diffusion in ILs focused on self-diffusivities,[16] the collective (or mutual) diffusion coefficient is required to describe mass transport in applications. Both experimental and simulation studies of mutual diffusion in ILs have mostly been concentrated on the infinite dilution regime where mutual and self-diffusivities become equal.[17−22] The concentration dependence of mutual diffusivities in systems with ILs has only been studied experimentally by Richter et al.[23] To

Received: April 1, 2011
Revised: May 27, 2011
Published: May 31, 2011

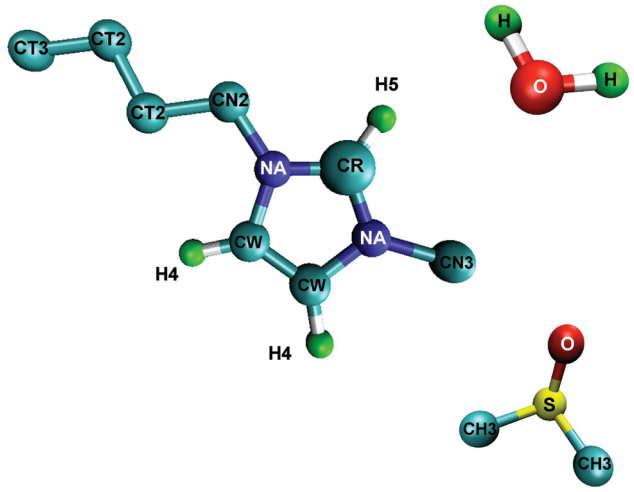

Figure 1. Schematic representation of the structure of $C_n mim^+$ cations (here, $n = 4$), dimethyl sulfoxide (DMSO), and water. The atom labeling for the IL is as follows: NA: N, CR: C, CW: C, H4: H, H5: H, CN3: CH_3, CN2: CH_2, CT2: CH_2, CT3: CH_3.

the best of our knowledge, a molecular understanding of the concentration dependence of transport diffusivities in ILs is still lacking.

Mutual diffusion is conveniently described using the Maxwell–Stefan (MS) theory. General interest in MS diffusivities increases as (1) they usually depend less on concentration than Fick diffusivities, and (2) the (electro)chemical potential gradient is used as the driving force of diffusion. In a system containing n components, $n(n-1)/2$ MS diffusivities are sufficient to describe mass transport, while $(n-1)^2$ Fick diffusivities are needed. The $(n-1)^2$ Fick diffusivities are therefore not independent. (3) In multicomponent systems, MS diffusivities can be predicted using the MS diffusivities obtained from binary mixtures. Multicomponent Fick diffusivities are not related to their binary counterparts, which hinders the development of predictive models for describing multicomponent mass transport. MS diffusion coefficients cannot be directly accessed in experiments but need to be derived from Fick diffusivities. Previously, we showed that MD simulations are a valuable tool for developing and testing predictive models for MS diffusivities.[15,24]

In this study, MD simulations have been performed in binary mixtures with 1-alkyl-3-methylimidazolium chloride ($C_n$mimCl, $n = 2, 4, 8$), DMSO (dimethyl sulfoxide), and H_2O. Our model is validated using experimental self-diffusivities. Self- and MS diffusivities in various binary mixtures are computed. We find the following: (1) Self- and MS diffusivities strongly decrease with increasing IL concentration. (2) Additions of H_2O or DMSO have a different influence on liquid structure: ILs stay in a form of isolated ions in $C_n$mimCl–H_2O mixtures; however, ion pairs are preferred in $C_n$mimCl-DMSO systems. (3) Recently, we proposed a new model for predicting MS diffusivities at infinite dilution based on the easily measurable self-diffusivities.[24] The only underlying assumption is that velocity cross-correlations are neglected. In the studied mixtures with ILs, our model results in large deviations in estimating MS diffusivities showing that velocity cross-correlations are important in systems with ILs.

This paper is organized as follows. In Section 2, we describe the procedure of obtaining diffusion coefficients from MD simulations as well as the simulation details. In Section 3, we review several predictive models which are often used for estimating the diffusion coefficients. The computed diffusivities and the quality of predictive models are analyzed in Section 4. Our conclusions are addressed in Section 5.

2. MOLECULAR DYNAMICS SIMULATIONS

2.1. Obtaining Diffusivities from MD Simulation. Equilibrium molecular dynamics (EMD) simulations are used to determine self- and MS diffusivities. The self-diffusivity describes the motion of individual molecules. The Einstein equation connects the self-diffusivity $D_{a,\mathrm{self}}$ of component a to its average molecular displacements[25]

$$D_{a,\mathrm{self}} = \frac{1}{6N_a}\lim_{n\to\infty}\frac{1}{n\cdot\Delta t}\left\langle\left(\sum_{l=1}^{N_a}\left(r_{l,a}(t+n\cdot\Delta t)-r_{l,a}(t)\right)^2\right)\right\rangle \tag{1}$$

Here, N_a is the total number molecules of component a, Δt is the integration time step in MD, n is the number of time steps, $r_{l,a}(t)$ is the position of l^{th} molecule of component a at time t. The mean squared displacement is updated with different frequencies according to the order-n algorithm described in refs 25 and 26. By plotting the mean squared displacements as a function of time on a log–log scale, we determined the diffusive regime and extracted the diffusivities. This is explained in Figure S1 of the Supporting Information.

MS diffusivities describe the friction between different components. In practice, the matrix of Onsager coefficients $[\Lambda]$ is computed, which can be obtained directly from EMD simulations using[27]

$$\Lambda_{ab} = \frac{1}{6}\lim_{n\to\infty}\frac{1}{N}\frac{1}{n\cdot\Delta t}\left\langle\left(\sum_{l=1}^{N_a}\left(r_{l,a}(t+n\cdot\Delta t)-r_{l,a}(t)\right)\right)\left(\sum_{k=1}^{N_b}\left(r_{k,b}(t+n\cdot\Delta t)-r_{k,b}(t)\right)\right)\right\rangle \tag{2}$$

In this equation, N is the total number of molecules in the simulation, and a and b are the molecule types. Note that the matrix $[\Lambda]$ is symmetric, that is, $\Lambda_{ab} = \Lambda_{ba}$. The MS diffusivities follow directly from the Onsager coefficients. Details are shown in the Supporting Information.

2.2. Details of EMD Simulation. To describe the interactions between atoms and molecules in the system, we used a classical force field approximation for the total potential energy U,

$$U = \sum_{\mathrm{bonds}} K_r(r-r_0)^2 + \sum_{\mathrm{angles}} K_\theta(\theta-\theta_0)^2 + \sum_{\mathrm{dihedrals}} K_\chi[1+\cos(n\chi-\delta)] + \sum_{i<j} 4\varepsilon_{ij}\left[\left(\frac{\sigma_{ij}}{r_{ij}}\right)^{12}-\left(\frac{\sigma_{ij}}{r_{ij}}\right)^{6}\right] + \sum_{i<j}\frac{1}{4\pi\varepsilon_0}\frac{q_i q_j}{r_{ij}} \tag{3}$$

in which K_r, K_θ, and K_χ are energy parameters for bond-stretching, bond-bending, and dihedrals, respectively; ε_{ij} and σ_{ij} are the energy and size parameters in the Lennard–Jones (LJ) potential, and q_i is the partial charge of (united) atom i. We use the united-atom approach for ILs and DMSO. CH_x groups are considered as single interaction centers with their own effective interaction potentials. Bead types H4 and H5 (see Figure 1) in the imidazolium ring are not treated as united atoms as they are more active and important for describing hydrogen bonding.[14] A flexible SPC model is used to describe water.[28] In this work, the

dx.doi.org/10.1021/jp203026c |J. Phys. Chem. B 2011, 115, 8506–8517

Table 1. Comparison of Experimental and Computed Densities and Self-Diffusivities of DMSO and H_2O at 1 atm[a]

DMSO				
	$\rho/(g\cdot cm^{-3})$		$D_{self}/(10^{-9}\ m^2\cdot s^{-1})$	
T/K	this work	experiment	$D_{self}^{this\ work}$	D_{self}^{exp}
298	1.090	1.096[57]	0.79	0.80[43]
303	1.082	1.091[57]	0.97	n.a.[b]
318	1.068	n.a.	1.30	1.07[58]
328	1.061	n.a.	1.40	1.26[58]
368	1.026	n.a.	2.38	n.a.
H_2O				
	$\rho/(g\cdot cm^{-3})$		$D_{self}/(10^{-9}\ m^2\cdot s^{-1})$	
T/K	this work	experiment	$D_{self}^{this\ work}$	D_{self}^{exp}
298	1.003	0.997[59]	3.00	2.49[43]
310	0.995	0.993[60]	3.70	3.07[61]
323	0.986	0.988[60]	4.69	3.95[61]
348	0.972	0.975[60]	6.12	6.08[61]
368	0.946	0.960[60]	8.40	n.a.

[a] The statistical errors of computed densities are less than 1% and less than 3% for the computed self-diffusivities. [b] Not available.

Table 2. Comparison of Experimental and Computed Densities of $C_n$mimCl at 1 atm[a]

C_1mimCl[b]				
	$\rho/(g\cdot cm^{-3})$		$D/(10^{-9}\ m^2\cdot s^{-1})$	
T/K	this work	experiment	$D_{+,self}$	$D_{-,self}$
400	1.119	1.140[62]	0.190	0.162
425	1.105	1.120[62]	0.298	0.258
C_2mimCl[c]				
	$\rho/(g\cdot cm^{-3})$		$D/(10^{-9}\ m^2\cdot s^{-1})$	
T/K	this work	experiment	$D_{+,self}$	$D_{-,self}$
368	1.105	n.a.[d]	0.109	0.074
373	1.098	1.11[62]	0.119	0.097
400	1.072	1.09[62]	0.247	0.210
C_4mimCl[e]				
	$\rho/(g\cdot cm^{-3})$		$D/(10^{-9}\ m^2\cdot s^{-1})$	
T/K	this work	experiment	$D_{+,self}$	$D_{-,self}$
353	1.048	n.a.	0.010	0.009
368	1.042	n.a.	0.027	0.026
373	1.033	n.a.	0.028	0.028
400	1.024	n.a.	0.079	0.070
C_8mimCl[f]				
	$\rho/(g\cdot cm^{-3})$		$D/(10^{-9}\ m^2\cdot s^{-1})$	
T/K	this work	experiment	$D_{+,self}$	$D_{-,self}$
368	0.989	n.a.	0.007	0.008
400	0.968	n.a.	0.037	0.039

[a] Computed self-diffusivities of ions are also listed. The statistical errors of computed densities are less than 1% and less than 4% for the computed self-diffusivities. [b] The melting point of C_1mimCl is 398−399 K; see refs 62 and 63. [c] The melting point of C_2mimCl is 357 K; see ref 62. [d] Not available. [e] The melting point of C_4mimCl is 314−339 K depending on the type of crystal polymorph; see ref 64. [f] The melting point of C_8mimCl is 285 K; see ref 51.

LJ potential is truncated and shifted at 12 Å. The Lorentz−Berthelot mixing rules are applied to calculate the LJ parameters for the interactions of unlike atoms.[29] Electrostatic interactions are handled by Ewald summation using a relative precision of 10^{-5}. Since the force fields for 1-alkyl-3-methylimidazolium, chloride [$C_n$mim][Cl], DMSO, and H_2O were fitted at different cutoff radii (see refs 14, 28, and 30), we fixed the cutoff radius for LJ interactions at r_{cut} = 12 Å and slightly adjusted the force field by keeping the size parameter σ constant and changing the energy parameter ε. We fit the force field to the experimental density at lower temperatures (5 °C above the melting points) as we feel that it is important that the simulations reproduce the experimental density.[15,24] The values of the force field parameters for nonbonded interactions are listed in Tables S1 and S2 of the Supporting Information; parameters for nonbonded interactions can be found in refs 14, 28, and 30. Pure component data at higher temperatures are well-reproduced and comparable with the experimental results as shown in Tables 1 and 2. Recently, Chen et al. used this force field for ILs to compute the viscosity of BmimCl and its mixture with water, acetonitrile, and glucose.[31] Their results showed reasonable agreement between simulations and experiments; that is, the computed viscosity of ILs is 20−50% larger than that obtained from experiments. Therefore, we should expect that our computed diffusivities of ILs are lower than in experiments. It is important to note that we are aiming to study the dependence of diffusivities on mixture composition instead of expanding the database of diffusion coefficients of ILs. Therefore, we feel that the force field applied in this work is sufficiently accurate for our purpose.

The simulations were carried out as follows: first, independent initial configurations are generated and equilibrated using EMD simulations in the NPT ensemble at the target temperature and pressure. The total number of molecules ranges from 100 (pure ILs) to 600 (pure water). The Nosé−Hoover thermostat and barostat are used with a time constants of 0.2 and 1 ps, respectively. Three-dimensional periodic boundary conditions consistent with a cubic box were applied to obtain properties corresponding to bulk systems. A time step of 1 fs is used for integrating the equation of motion. When the average density of the systems does not change with time, we use the equilibrated system at this average density for computing the self- and MS diffusivities in the microcanonical (NVE) ensemble. Simulations longer than 100 ns are often needed to obtain accurate diffusivities; see Figure S1 of the Supporting Information.

3. PREDICTIVE MODELS FOR DIFFUSION

3.1. Maxwell−Stefan Diffusivities. The MS formulation uses (electro)chemical potential gradients as driving forces for mass

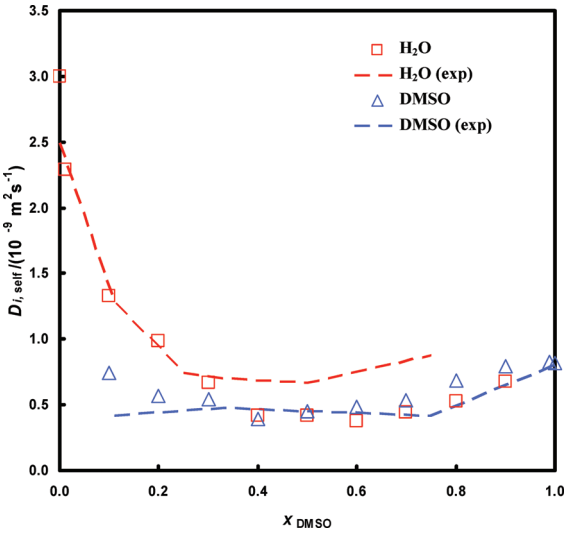

Figure 2. Computed self-diffusivities of DMSO−H_2O mixtures at 298 K, 1 atm. Open symbols represent simulation results, and dashed lines represent experimental data.[43] The error bars of computed diffusivities are smaller than the symbol size.

transport. For liquid mixtures at constant temperature and pressure, in the absence of external electric fields the MS equation equals[32,33]

$$\sum_{j=1}^{n-1} \Gamma_{ij} \nabla x_j = \sum_{\substack{k=1 \\ k \neq i}}^{n} \frac{x_i J_k - x_k J_i}{c_t Đ_{ik}} \tag{4}$$

where Γ_{ij} is the thermodynamic factor. $Đ_{ij}$ represent the MS diffusivity describing the friction between components i and j. MD simulations can be used to directly compute the MS diffusivities $Đ_{ij}$ from local particle fluctuations as shown in Section 2. It is important to note that MS diffusivities do depend on the concentration.[27] For ordinary electrolyte solutions, the concentration dependence has usually been studied from infinite dilution to the solubility limit. Convenient prediction models covering the full concentration range are lacking. For mixtures of organic compounds, the Vignes equation is often recommended to predict the concentration dependence of MS diffusivities.[34,35] In a binary electrolyte solution, the generalized Vignes equation becomes

$$\begin{aligned} Đ_{+-} &= (Đ_{+-}^{x_+ \to 1})^{x_+} (Đ_{+-}^{x_- \to 1})^{x_-} (Đ_{+-}^{x_k \to 1})^{x_k} \\ Đ_{+k} &= (Đ_{+k}^{x_+ \to 1})^{x_+} (Đ_{+k}^{x_- \to 1})^{x_-} (Đ_{+k}^{x_k \to 1})^{x_k} \\ Đ_{-k} &= (Đ_{-k}^{x_+ \to 1})^{x_+} (Đ_{-k}^{x_- \to 1})^{x_-} (Đ_{-k}^{x_k \to 1})^{x_k} \end{aligned} \tag{5}$$

in which the subscripts + and − represent the cation and anion of the IL respectively. k represents a component carrying no net charge. It is important to note that eq 5 is a valid mathematical operation even though it is physically impossible, as it violates electroneutrality; that is, $Đ_{ij}^{x_+ \to 1}$ and $Đ_{ij}^{x_- \to 1}$ do not exist. To preserve electroneutrality, we rewrite the Vignes equation as

$$\begin{aligned} Đ_{+-} &= (Đ_{+-}^{x_{IL} \to 1})^{x_{IL}} (Đ_{+-}^{x_k \to 1})^{x_k} \\ Đ_{+k} &= (Đ_{+k}^{x_{IL} \to 1})^{x_{IL}} (Đ_{+k}^{x_k \to 1})^{x_k} \\ Đ_{-k} &= (Đ_{-k}^{x_{IL} \to 1})^{x_{IL}} (Đ_{-k}^{x_k \to 1})^{x_k} \end{aligned} \tag{6}$$

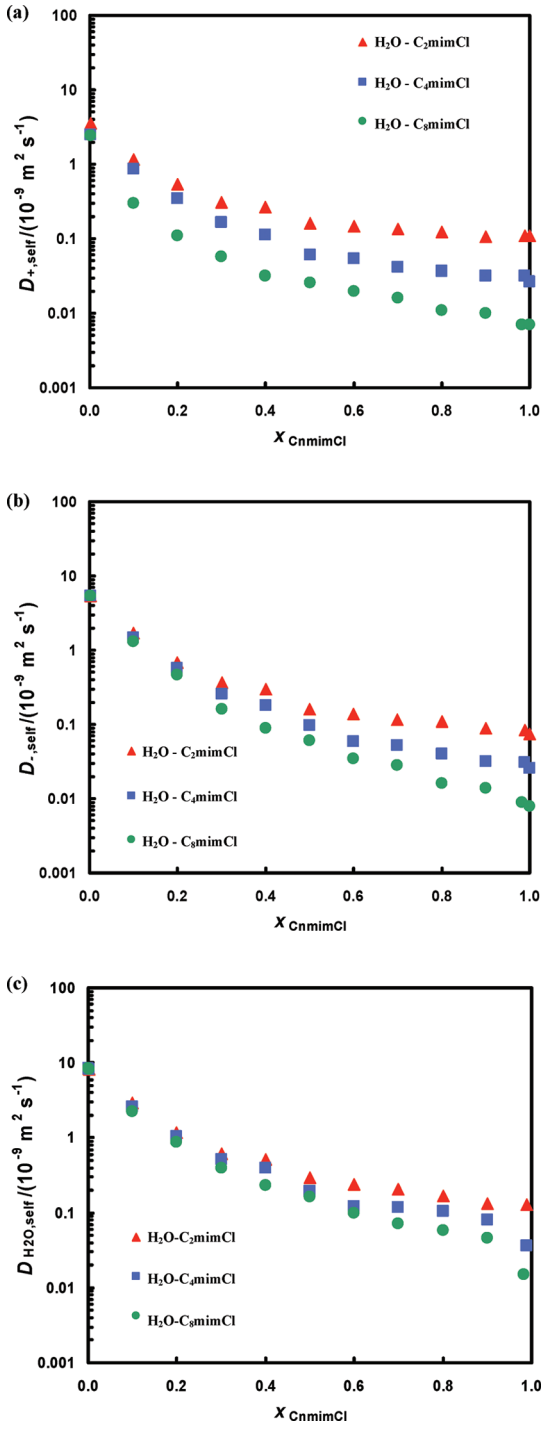

Figure 3. Computed self-diffusivities of $C_n$mimCl−H_2O mixtures at 368 K, 1 atm. (a) Self-diffusivity of $C_n mim^+$; (b) self-diffusivity of Cl^-; (c) self-diffusivity of H_2O. The error bars of computed diffusivities are smaller than the symbol size.

in which x_{IL} is the number of IL molecules divided by the total number of molecules in the system (IL + solvent). Therefore

$$x_{IL} + x_k = 1 \tag{7}$$

in which x_k is the mole fraction of the uncharged component k.

3.2. Maxwell−Stefan Diffusivities at Infinite Dilution. Equation 6 requires the value of $Đ_{+-}^{x_k \to 1}$ (or $Đ_{ij}^{x_k \to 1}$) which describes

dx.doi.org/10.1021/jp203026c |J. Phys. Chem. B 2011, 115, 8506–8517

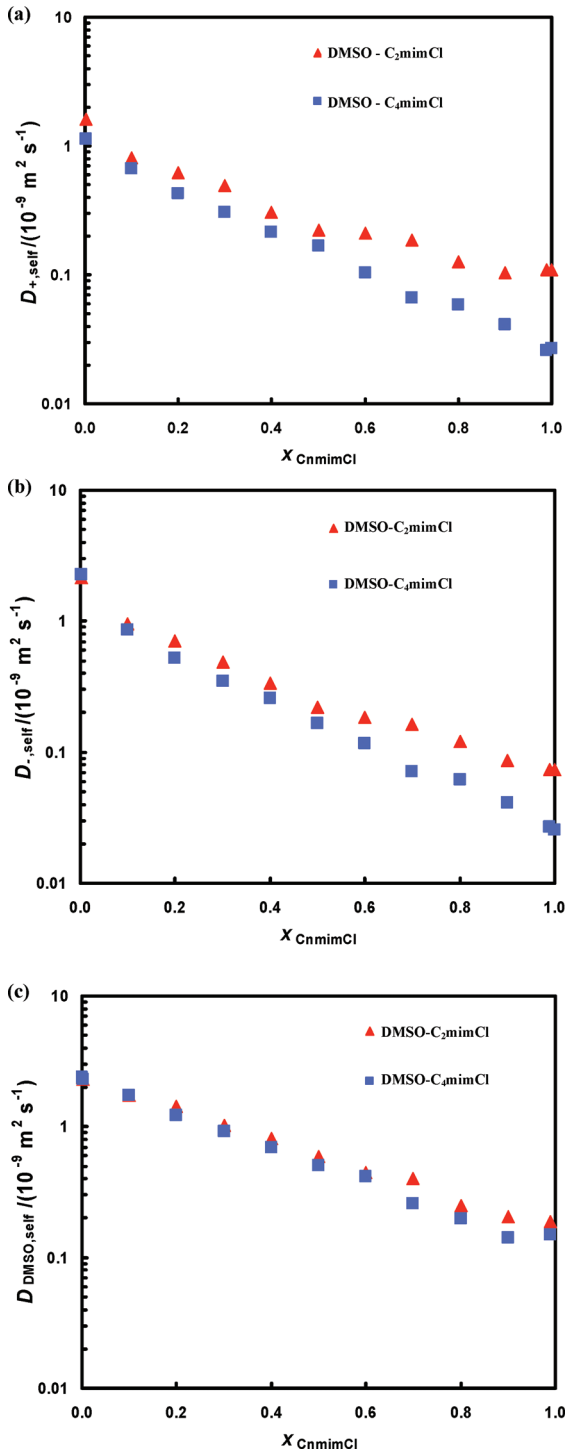

Figure 4. Computed self-diffusivities of $C_n$mimCl−DMSO mixtures at 368 K, 1 atm. (a) Self-diffusivity of $C_n$mim$^+$; (b) self-diffusivity of Cl^-; (c) self-diffusivity of DMSO. The error bars of computed diffusivities are smaller than the symbol size.

the friction between cation and anion when both are infinitely diluted in solvent k. This quantity is not easily accessible in experiments as no direct measurement is possible.[36] In the past decades, several empirical models were proposed for estimating the quantity $Đ_{ij}^{x_k \to 1}$. However, all of them are lacking a sound theoretical basis.[27,37−40]

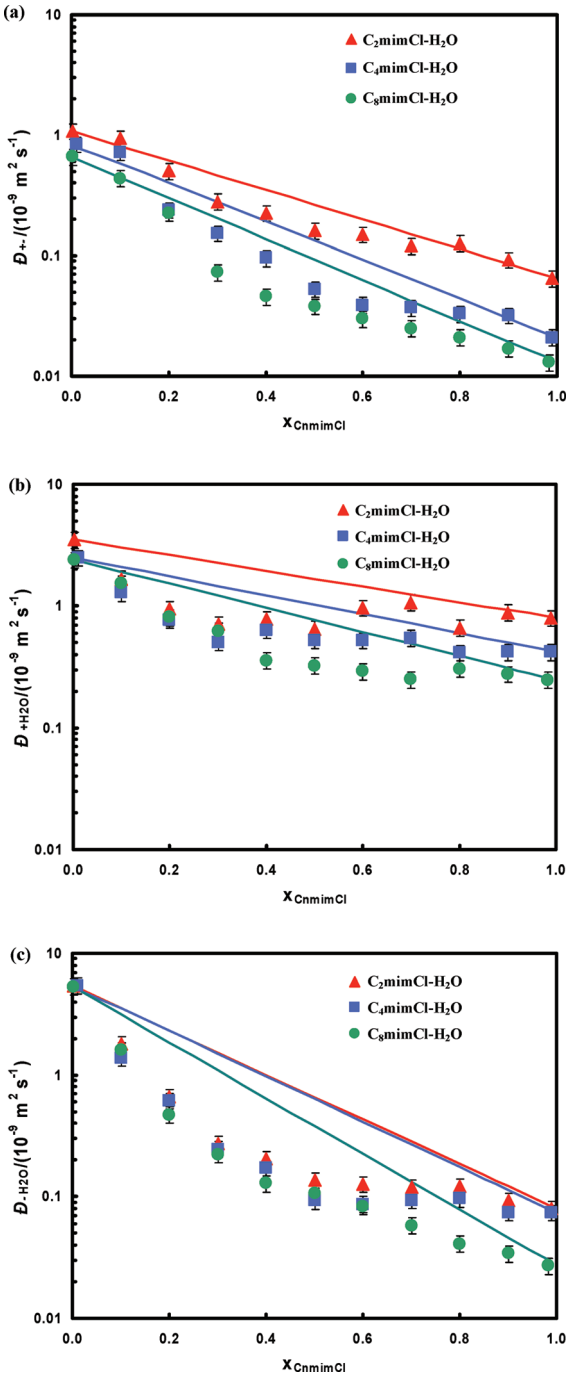

Figure 5. MS diffusivities of $C_n$mimCl−H_2O mixtures at 368 K, 1 atm. (a) $Đ_{+-}$; (b) $Đ_{+H_2O}$; (c) $Đ_{-H_2O}$. The solid lines are the predicted MS diffusivities using eq 6.

Recently, we have showed that $Đ_{ij}^{x_k \to 1}$ does exist (i.e., does not depend on the ratio x_i/x_j) and we have developed a new predictive model for $Đ_{ij}^{x_k \to 1}$ based on the linear response theory and the Onsager relations.[24] We find that $Đ_{ij}^{x_k \to 1}$ can be expressed in terms of self-diffusivities and integrals over velocity cross-correlation functions.[24]

$$Đ_{ij}^{x_k \to 1} = \frac{D_{i,\mathrm{self}}^{x_k \to 1} \cdot D_{j,\mathrm{self}}^{x_k \to 1}}{D_{k,\mathrm{self}}^{x_k \to 1} + C_x} \qquad (8)$$

dx.doi.org/10.1021/jp203026c |J. Phys. Chem. B 2011, 115, 8506–8517

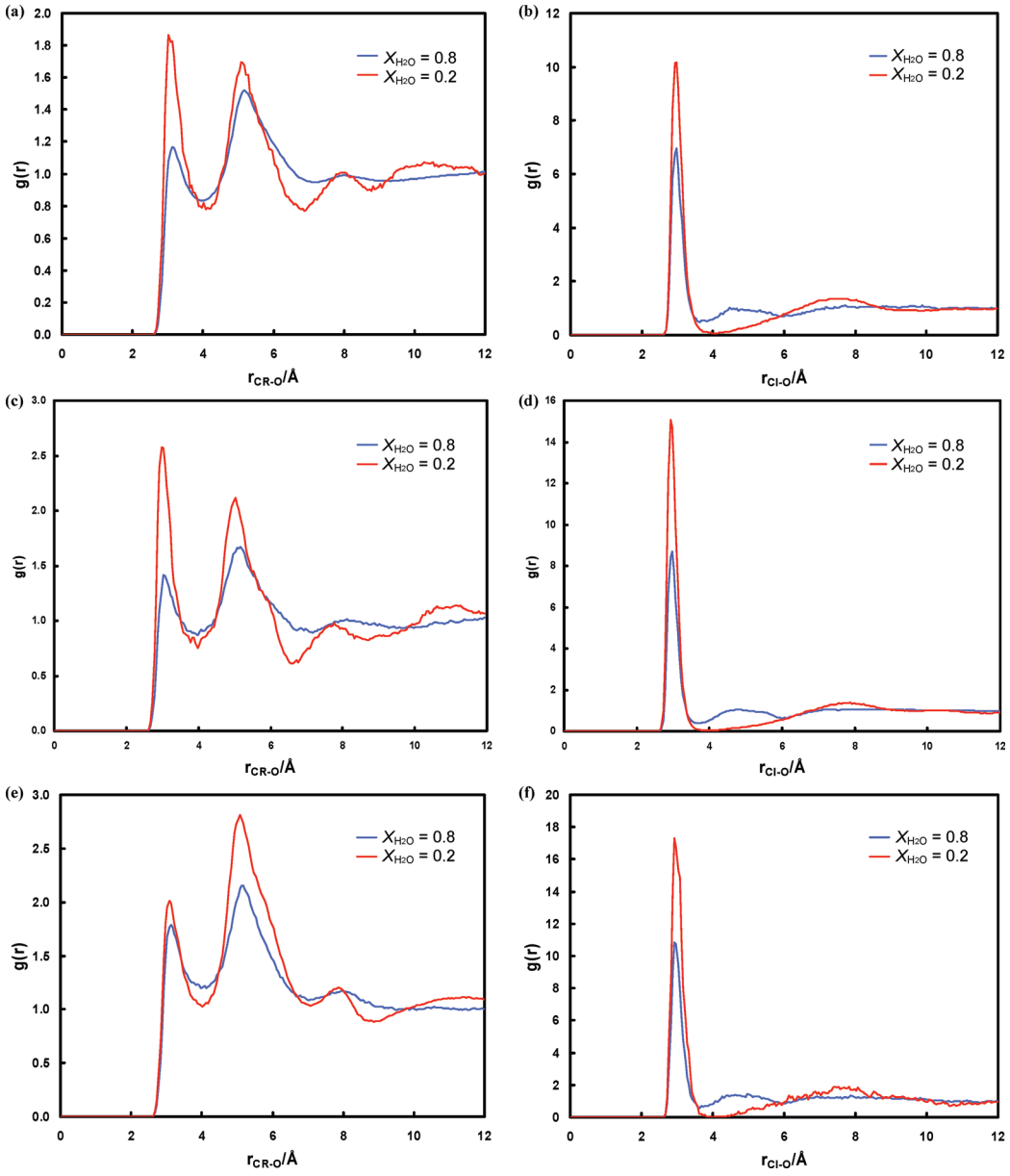

Figure 6. RDFs of CR−O and Cl−O atom pairs in water at 368 K, 1 atm. (a) CR−O in a C_2mimCl−water mixture. CR is an atom of the cation, see Figure 1; (b) Cl−O in a C_2mimCl−water mixture; (c) CR−O in a C_4mimCl−water mixture; (d) Cl−O in a C_4mimCl−water mixture; (e) CR−O in a C_8mimCl−water mixture; (f) Cl−O in a C_8mimCl−water mixture.

with $D_{i,\mathrm{self}}$ is the self-diffusivity of component i. The parameter C_x is related to integrals over velocity cross-correlation functions; see ref 24. We assumed that in the limit of infinite dilution (here, we consider a case in which components i and j are infinitely diluted in component k), the correlation of molecules that are of type k is much larger than the correlation of unlike molecules, that is, $C_x/D_{k,\mathrm{self}} \approx 0$. By neglecting the integrals over velocity cross-correlation functions, we obtain a convenient predictive model for $Đ_{ij}^{x_k \to 1}$

$$Đ_{ij}^{x_k \to 1} = \frac{D_{i,\mathrm{self}}^{x_k \to 1} \cdot D_{j,\mathrm{self}}^{x_k \to 1}}{D_{k,\mathrm{self}}^{x_k \to 1}} \qquad (9)$$

It was shown in ref 24 that eq 9 is superior compared to the existing models in several systems, that is, systems in which particles interacting using Weeks−Chandler−Andersen (WCA) potential or ternary mixtures of *n*-hexane−cyclohexane−toluene. In the ethanol−methanol−water system, eq 9 deviates from direct calculations of $Đ_{ij}$ revealing that velocity cross-correlation functions should be taken into account as C_x is of the same order of magnitude as $D_{k,\mathrm{self}}^{x_k \to 1}$. This deviation is mainly due to the formation of hydrogen bonds. In this work, we also test the ability of eq 9 in predicting $Đ_{ij}^{x_k \to 1}$ in mixtures with ILs.

3.3. Salt Diffusivity. The electroneutrality condition forces both ions of ILs to diffuse at the same speed in the absence of an electric current. This phenomenon is known as salt diffusion. It is well-known that the correct driving force for diffusion is the electrochemical

dx.doi.org/10.1021/jp203026c |*J. Phys. Chem. B* 2011, 115, 8506–8517

potential gradient. The MS diffusion coefficient of IL molecules based on a thermodynamic driving force is defined as[41]

$$Đ_{IL} = \frac{Đ_{+k}Đ_{-k}(z_+ - z_-)}{z_+Đ_{+k} - z_-Đ_{-k}} \quad (10)$$

with z is the charge number of the ion. $Đ_{+k}$ and $Đ_{-k}$ are defined by eq 4. The often used salt diffusivity D_{IL} which considers the concentration gradient as the driving force of diffusion can be related to $Đ_{IL}$ using[41]

$$D_{IL} = Đ_{IL}\frac{c_T}{c_0}\left(1 + \frac{d \ln \gamma_{+-}}{d \ln m}\right) \quad (11)$$

where γ_{+-} is the mean molal activity coefficient. In this equation, m is the molarity (moles of electrolyte per kilogram of solvent), c_T is the total solution concentration ($mol \cdot m^{-3}$), and c_0 is the concentration of the solvent ($mol \cdot m^{-3}$). In the limit of infinite dilution, the expression for the salt diffusivity D_{IL} can be simplified as[41]

$$D_{IL} = \frac{D_{+,self}D_{-,self}(z_+ - z_-)}{z_+D_{+,self} - z_-D_{-,self}} \quad (12)$$

4. RESULTS AND DISCUSSION

4.1. Model Validation via Self-Diffusivities. *4.1.1. Pure ILs.* Table 2 shows the computed self-diffusivities of $C_n$mimCl at 1 atm. Simulations were carried out above the melting points of $C_n$mimCl. The results shown in Table 2 can be summarized as follows: (1) As the temperature increases, self-diffusivities of $C_n$mimCl increase as well. This is due to both decreased density and enhanced mobilities of molecules. (2) For $C_n$mimCl with a shorter tail, that is, $n = 1, 2$, the self-diffusivity of cations is larger than that of anions. (3) As the side chain increases, the self-diffusivities of cation and anion are almost equal. This is in agreement with the observations by Feng et al.[42]

4.1.2. H_2O–DMSO. Figure 2 compares self-diffusivities in the DMSO–H_2O system obtained from both simulations and experiments.[43] A strong nonideal behavior of the mixture was observed due to the strong hydrogen bond between DMSO and H_2O. The smallest values for self-diffusivities of both components were found between $x_{DMSO} = 0.4–0.6$. Moreover, it is clear that the dynamics of water is more strongly affected than that of DMSO. A similar feature has been observed in both experiments and simulations.[44,45] A general understanding of the structure of water–DMSO mixtures was derived earlier mainly from X-ray, neutron scattering, and computer simulations.[46−49] It is well-established that the local minimum in Figure 2 is due to the formation of 1:DMSO–2:H_2O or 2:DMSO–1:H_2O rigid structures which restrict the mobility of molecules yielding lower self-diffusivities.[43−45] In the range $x_{DMSO} < 0.4$ or $x_{DMSO} > 0.6$, excess water molecules and DMSO molecules are available which are less restricted by these rigid structures. This results in larger self-diffusivities.

4.1.3. IL–H_2O. Experimental studies have shown that $C_n$mimCl (n = 2, 4, 8) is completely miscible with H_2O at 368 K, 1 atm.[50,51] Figure 3 shows self-diffusivities of $C_n mim^+$, Cl^-, and H_2O in IL–H_2O mixtures. The self-diffusivities of all components strongly decrease with an increasing concentration of ILs. For the self-diffusivities of anions and H_2O, two regimes are formed. At lower IL concentration, the influence of the size of cation on self-diffusivity is negligible. As the IL concentration increases, the influence originating from the cation size becomes important. Because of the two regimes, deviations from a single exponential behavior are observed for self-diffusivities in IL–H_2O mixtures. Strongly decreasing self-diffusivities with increasing IL concentration were observed in several other studies.[10,42] Lovell et al. measured self-diffusivities in 1-ethyl-3-methyl-imidazolium acetate cellulose solutions using ^{1}H NMR.[10] Feng et al. computed the self-diffusivities in $C_n$mimCl–H_2O and $C_n$mimBF_4–H_2O mixtures using MD simulations.[42] These authors found that an exponential relation is the best description for the concentration dependence of the self-diffusivities of ions.

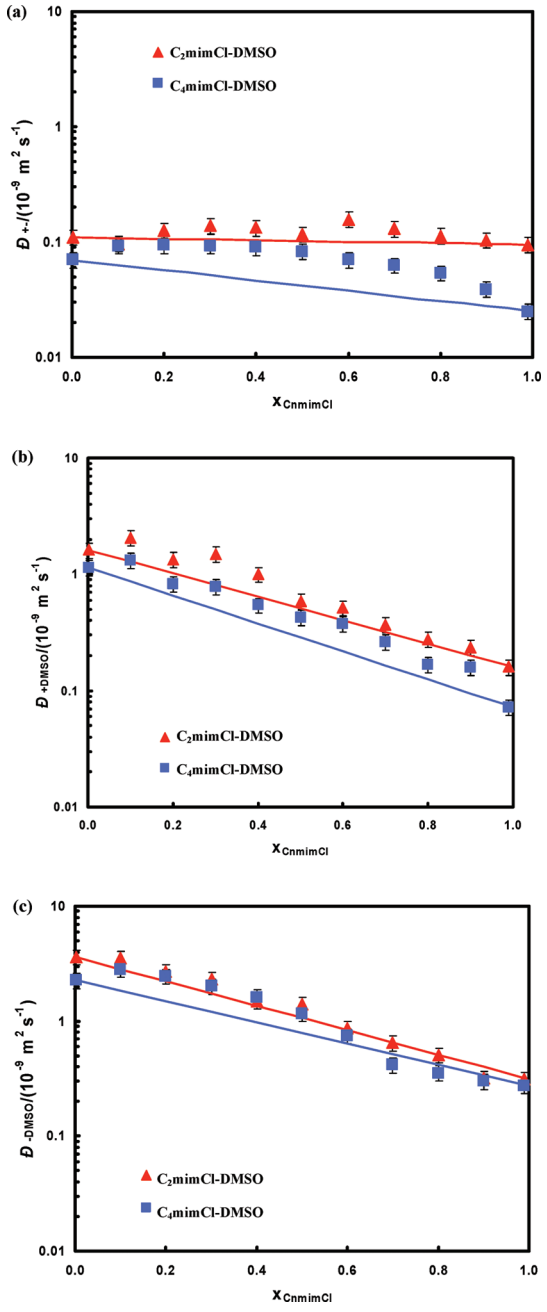

Figure 7. MS diffusivities in $C_n$mimCl–DMSO mixtures at 368 K, 1 atm. (a) $Đ_{+-}$; (b) $Đ_{+DMSO}$; (c) $Đ_{-DMSO}$. The solid lines are the predicted MS diffusivities using eq 6.

4.1.4. IL–DMSO. Figure 4 shows the self-diffusivities in $C_n$mimCl–DMSO mixtures. We only studied $C_n$mimCl–DMSO systems with n = 2, 4. The C_8mimCl–DMSO system is not included in this

dx.doi.org/10.1021/jp203026c |J. Phys. Chem. B 2011, 115, 8506–8517

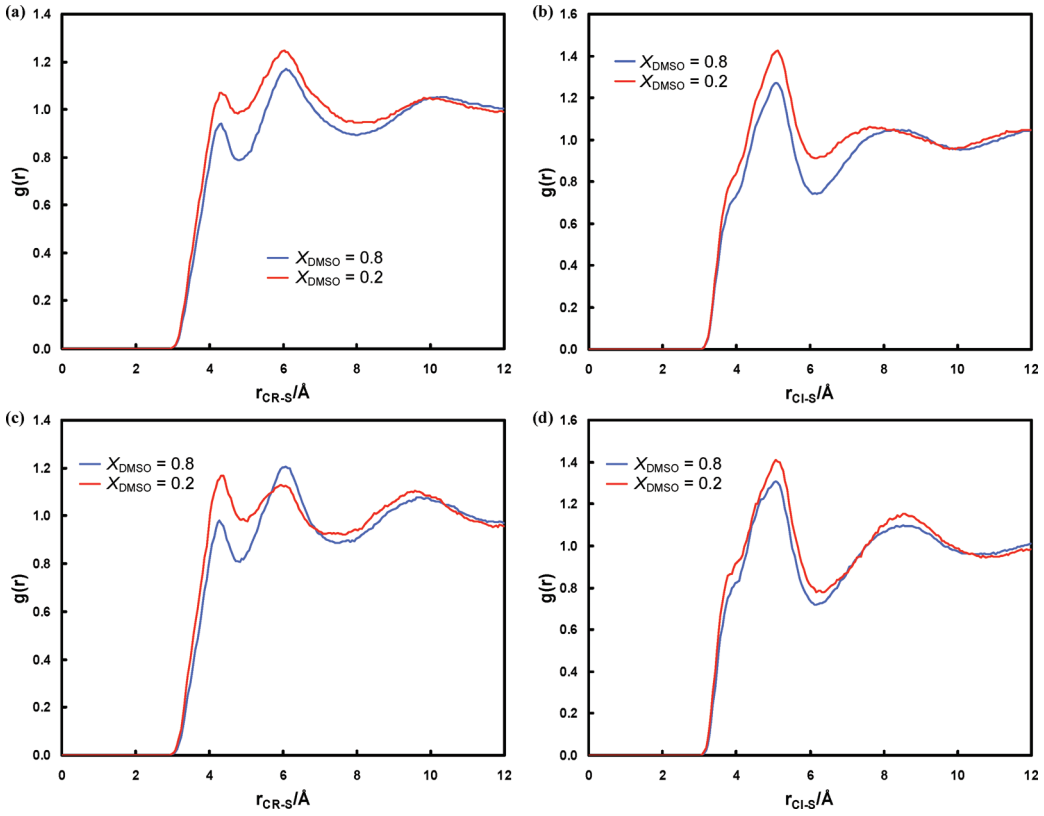

Figure 8. RDF of CR−S and Cl−S atom pairs in DMSO at 368 K, 1 atm. (a) CR−S in a C_2mimCl−DMSO mixture. CR is an atom of the cation, see Figure 1; (b) Cl−S in a C_2mimCl−DMSO mixture; (c) CR−S in a C_4mimCl−DMSO mixture (CR is an atom on cation, see Figure 1); (d) Cl−S in a C_4mimCl−DMSO mixture.

study as the solubility of C_8mimCl in DMSO is not known. For $C_n$mimCl−DMSO systems, self-diffusivities exponentially decrease with increasing IL concentration. However, the decrease of self-diffusivities in $C_n$mimCl−DMSO mixtures is less pronounced than that in IL aqueous solutions.

The observations from Figures 3 and 4 can be summarized as follows: (1) the self-diffusivities of all components decrease strongly as the ILs concentration increases; (2) larger cations result in smaller self-diffusivities; (3) the side chain length of cations plays a minor role in determining the self-diffusivities in the IL−DMSO systems. The values of the computed diffusivities in these figures are listed in Tables S3 and S4 of the Supporting Information.

4.2. Maxwell-Stefan Diffusivities and Radial Distribution Functions. *4.2.1. IL−H_2O.* Figure 5 shows the MS diffusivities $Đ_{+-}$, $Đ_{+H_2O}$, and $Đ_{-H_2O}$ in $C_n$mimCl−H_2O mixtures. It is clear that (1) both $Đ_{+-}$ and $Đ_{-H_2O}$ decrease with the increasing IL concentration, and (2) $Đ_{+H_2O}$ is less sensitive to the concentration compared to $Đ_{+-}$ and $Đ_{-H_2O}$. (3) At the same water content, the MS diffusivities are smaller in a system containing larger IL molecules. As MS diffusivities can be considered as inverse friction coefficients (see eq 4), this implies stronger effective interactions between different components. (4) Also, the Vignes equation (eq 6) does not describe the simulation data very well. In all systems, lower diffusivities than predicted by the Vignes equation are observed.

Radial distribution functions (RDFs) characterize the liquid structure and can be used to understand trends in values of the diffusivities. Figure 6a,c,e shows the RDFs of CR−O (CR being an atom on the cation, see Figure 1; O is the oxygen atom in H_2O) in a $C_n$mimCl−H_2O mixture. In IL-rich mixtures, that is, x_{H_2O} = 0.2, the peak of the RDFs first increases with the increasing tail length of cations, followed by a decrease. In water-rich mixtures, that is, x_{H_2O} = 0.8, a continuous increasing trend of this peak was observed. Figure 6b,d,f shows the RDFs of Cl−O in $C_n$mimCl−H_2O mixtures. Much higher peaks were found compared to the RDFs of CR−O indicating a much stronger interaction (also due to less steric hindrance) between anions and water.

4.2.2. IL−DMSO. Figure 7 presents the MS diffusivities in $C_n$mimCl−DMSO mixtures with n = 2, 4. We observe that (1) $Đ_{+-}$ is not sensitive to the mixture composition meaning that adding DMSO has a negligible effect on the interaction or friction between cations and anions, (2) both $Đ_{+DMSO}$ and $Đ_{-DMSO}$ are larger than $Đ_{+-}$ indicating the cation−anion interaction is the most strongest, and (3) $Đ_{+DMSO}$ and $Đ_{-DMSO}$ are decreasing with increased IL concentration. The Vignes equation gives a better description of the concentration dependence than for the IL−H_2O system, but systematic deviations are still discernible.

Figure 8 shows the RDFs of CR−S and Cl−S (CR is an atom on cation; S is the sulfur atom in DMSO). Similar coordination numbers were observed for both CR−S and Cl−S which is different from the RDFs in IL aqueous solution. This similar trend for CR−S and Cl−S suggests that the interaction between cation and DMSO is comparable with that of the anion and DMSO.

4.2.3. Ionization of ILs. Figure 9 compares the RDFs between cations and anions in $C_n$mimCl−H_2O and $C_n$mimCl−DMSO mixtures. In the $C_n$mimCl−H_2O system, the first peak is reduced

dx.doi.org/10.1021/jp203026c |J. Phys. Chem. B 2011, 115, 8506–8517

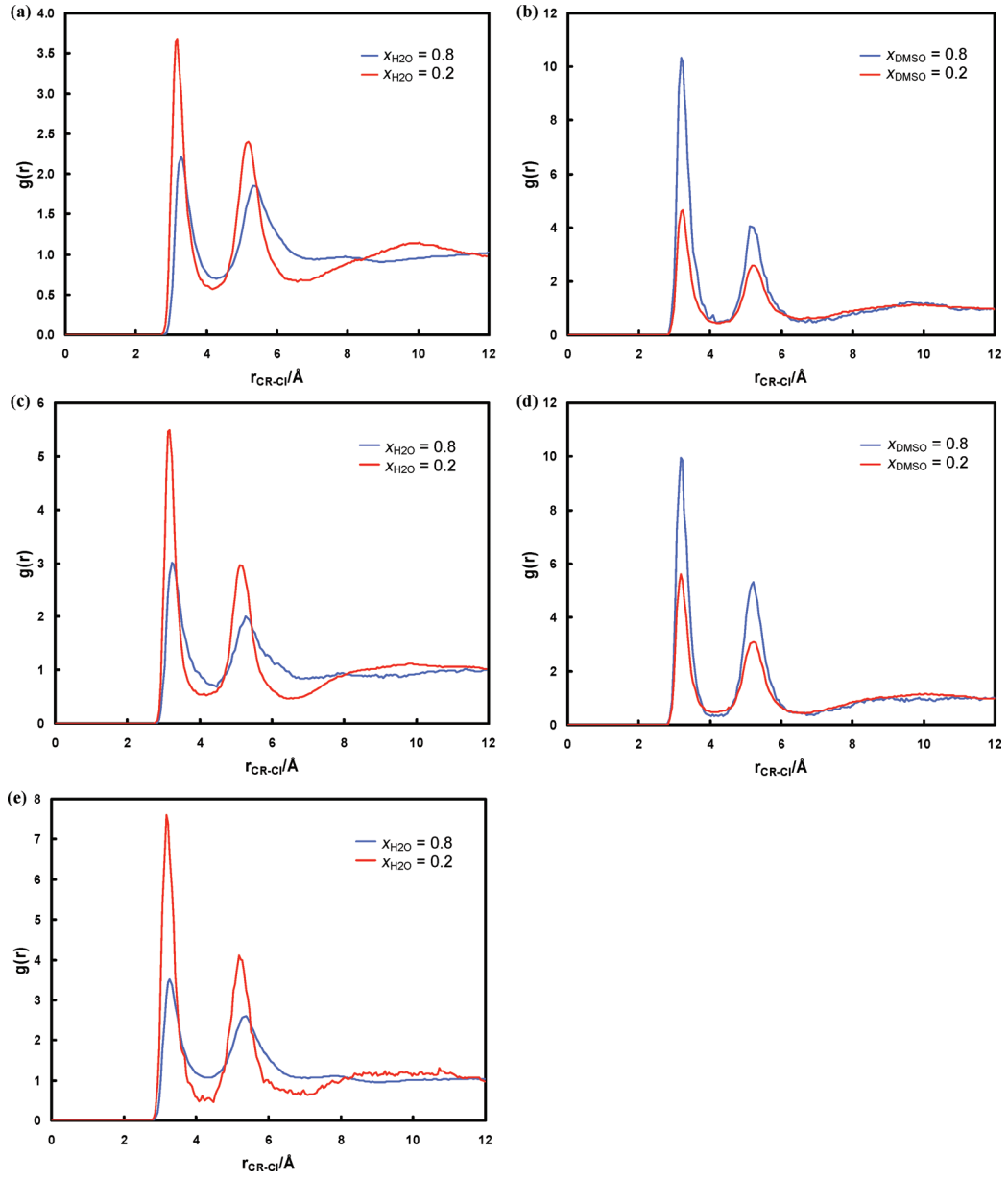

Figure 9. RDF of CR−Cl atom pairs in a binary mixture of $C_n$mimCl and water/DMSO at 368 K, 1 atm. (a) CR−Cl in a C_2mimCl−water mixture; (b) CR−Cl in a C_2mimCl−DMSO mixture; (c) CR−Cl in a C_4mimCl−water mixture; (d) CR−Cl in a C_4mimCl−DMSO mixture. (e) CR−Cl in a C_8mimCl−water mixture. CR is an atom of the cation, see Figure 1.

as the water concentration increases, as shown in Figure 9a,c,e, suggesting that the interaction between cations and anions is reduced. This reduced cation−anion interaction is due to the dilution by water. In other words, water molecules replace anions around the cations. The opposite behavior was observed for $C_n$mimCl−DMSO mixtures; a dramatic increase of the first peak was observed with the increased DMSO concentration, as shown in Figure 9b,d. This result suggests that the interaction between cations and anions is strengthened with increasing DMSO concentration.

$C_n$mimCl is miscible with both water and DMSO, but there are clear differences: $C_n$mimCl dissolves in water in the form of isolated ions. The results of Figure 9 suggest that, in the case of DMSO, $C_n$mimCl dissolves in a form of ion pairs. It would be very interesting to investigate the lifetime of these ion pairs in more detail.[52] A similar phenomenon was observed in both MD simulations and NMR measurement for a binary mixture with C_4mimCl.[50] This feature has been proposed for explaining a phenomenon observed previously in dissolving biopolymers using ILs.[50] IL−biopolymer systems are highly viscous. Therefore, a second solution is often added to reduce the viscosity. Experimental studies show that, by adding water, the ability of ILs for dissolving biopolymers is dramatically reduced.[53] In contrast, adding DMSO has a negligible effect on the dissolution of biopolymers.[50]

4.2.4. MS Diffusivities at Infinite Dilution. In the limit of infinite dilution, MS diffusivity $\mathcal{D}_{+-}^{x_k \to 1}$ can be obtained from both MD simulations and eq 9 as shown in Table 3. Equation 9 is parametrized using self-diffusivities which are listed in Table S5 of the Supporting Information. Absolute differences between

dx.doi.org/10.1021/jp203026c |J. Phys. Chem. B 2011, 115, 8506–8517

Table 3. Diffusivities of ILs Infinitely Diluted in H_2O or DMSO at 368 K, 1 atm[a]

$i-j$	$Đ_{+-}^{MD}$	$Đ_{+-}^{prediction}$	AD[b]
$C_2mimCl-H_2O$	1.08	2.29	112%
$C_4mimCl-H_2O$	0.84	1.65	96%
$C_8mimCl-H_2O$	0.56	1.55	177%
$C_2mimCl-DMSO$	0.11	2.46	2140%
$C_4mimCl-DMSO$	0.07	1.08	1446%

[a] Comparison between MS diffusivities obtained from MD simulations and the predictive model (eq 9). [b] Absolute difference normalized with corresponding result from MD simulations.

MD simulations and predictions were calculated to evaluate the quality of eq 9. We found that: (1) eq 9 overestimates the MS diffusivity $Đ_{+-}^{x_k \to 1}$; (2) eq 9 results in a large deviations in IL−DMSO mixtures. As discussed in ref 24, in mixtures with non- or weakly associated molecules, eq 9 is accurate and superior to the existing predictive models; in mixtures with highly associated molecules, eq 9 either overestimates or underestimates the MS diffusivity at infinite dilution. The assumption that the correlation of unlike molecules is negligible does not hold in these systems. Detailed information of velocity cross-correlations should then be taken into account. In this work, we found that the largest deviation occurred in IL−DMSO mixtures. This is mainly due to the increasing interaction between cations and anions in the presence of DMSO. In the IL−water mixtures, this interaction between ions is greatly reduced, yielding relatively smaller deviations. The information of velocity cross-correlation function in the studied mixtures is listed in Table S6 of the Supporting Information.

4.3. Diffusivity of IL Molecules. As mentioned previously, the electroneutrality condition forces both ions of ILs to diffuse at the same speed in the absence of an electric current. This phenomenon is known as salt diffusion. The MS diffusion coefficient of IL molecules $Đ_{IL}$ based on a thermodynamic driving force are calculated using eq 10 and presented in Figure 10. Not surprisingly, in IL−H_2O mixtures, the concentration dependence of $Đ_{IL}$ is in between the one found for $Đ_{+H_2O}$ and $Đ_{-H_2O}$. The IL MS diffusivity in water shows a strong, nontrivial dependence on the IL concentration. The influence of the alkyl chain length on the IL MS diffusion coefficient, however, is minor and for $x_{IL} < 0.5$ even negligible.

Sarraute et al. measured the Fick diffusivities of $C_4mimCl-H_2O$ mixtures at infinite dilution using the Taylor dispersion technique at temperatures ranging from 283 to 333 K.[17] According to the Arrhenius relation given by these authors, the value of the Fick diffusivity of IL molecules can be extrapolated to 368 K, resulting in a value 4.3×10^{-9} m^2 s^{-1}. Here, the calculated MS diffusivity of IL molecules is 4.0×10^{-9} m^2 s^{-1} for the same system. At infinite dilution, the thermodynamic factor equals one revealing an excellent agreement between the computed diffusivity and experimental data. Recall that the computed diffusivity of pure H_2O is larger than the experimental data while the computed diffusivities of ILs are expected to be lower than experimental results. The latter is because the molecular model results in overpredictions of the viscosity.[31] These deviations from experimental data are thus compensated in IL−H_2O systems, yielding a good agreement between computed and measured diffusivities.

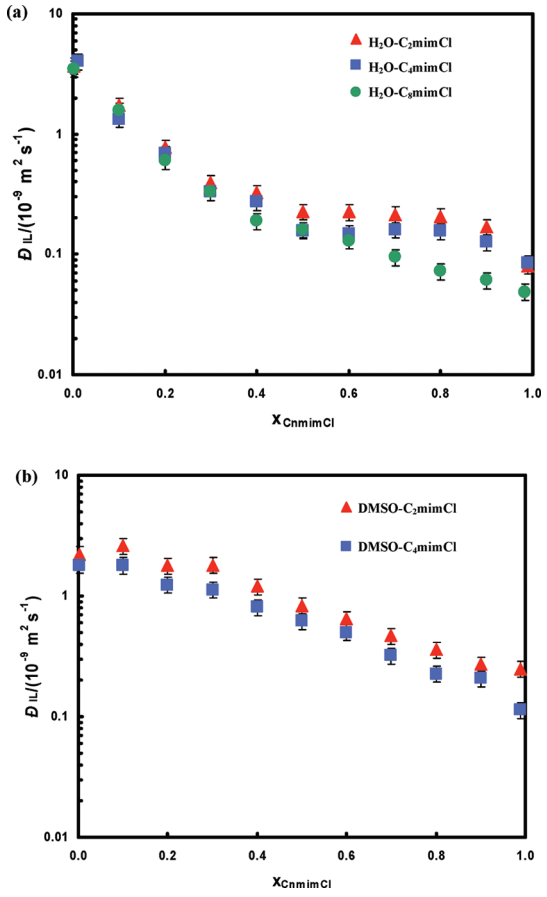

Figure 10. MS diffusivities of IL molecules in $C_n$mimCl−H_2O and $C_n$mimCl−DMSO mixtures at 368 K, 1 atm. (a) $Đ_{IL}$ in $C_n$mimCl−H_2O; (b) $Đ_{IL}$ in $C_n$mimCl−DMSO.

In the IL−DMSO systems, the decrease of $Đ_{IL}$ is comparable to that of $Đ_{+DMSO}$ and $Đ_{-DMSO}$. Again, the length of the alkyl chain in the IL does not influence the diffusion coefficient in the studied IL−DMSO mixtures. The data in Figure 10 are listed in Tables S3 and S4 of the Supporting Information.

For obtaining the salt diffusivity D_{IL}, it is essential to know the thermodynamic factor. The thermodynamic factor can be measured in experiments, that is, Karl Fischer titration.[54] However, difficulties still exist in implementing these methods. For example, the uncertainty in measured activity coefficient is 20% in a BmimCl−H_2O mixture.[54] Since the thermodynamic factor requires the concentration derivative of the activity coefficient, even larger errors have to be expected. In our view, MD simulations are thus the preferred method to study the behavior of MS diffusivities.

5. CONCLUSIONS

ILs are often considered as green solvents and good candidates for many processes. Their physical and chemical properties can be well-tuned through varied combinations of cations and anions. Imidazolium-based ILs are extensively studied in both experiments and computer simulations as they have been employed in practice, that is, as gas storage fluids and as separation medium.[55,56]

To the best of our knowledge, MS diffusivities in the mixtures with ILs have not yet been reported. In this study, we computed MS diffusivities using MD simulations in $C_n$mimCl−H_2O (n = 2, 4, 8) and $C_n$mimCl−DMSO mixtures (n = 2, 4). The effects of

alkyl chain length and mixture composition on the diffusion coefficients are explored. Our results show the following: (1) Self- and MS diffusivities strongly decrease with the increasing concentration of ILs. (2) The MS diffusivities of the ionic liquid ($Đ_{IL}$) are almost independent of the alkyl chain length. In particular, the dependency is much smaller than for the self-diffusivities indicating the necessity for studying mutual diffusion in detail. (3) The addition of H_2O and DMSO have a different influence on the liquid structure of ILs. ILs stay in a form of isolated ions in $C_n$mimCl−H_2O mixtures; however, ion pairs are preferred in $C_n$mimCl−DMSO systems. (4) In the limit of infinite dilution, MS diffusivity $Đ_{ij}^{x_i\to 1}$ can be predicted by eq 9 based on easily obtained self-diffusivities. In the studied mixtures with ILs, eq 9 results in larger deviations in estimating MS diffusivity suggesting that velocity cross-correlations are important. At present, no analytical or empirical methods are available to estimate these velocity cross-correlations, and one has to rely on molecular simulation.

■ ASSOCIATED CONTENT

Supporting Information. Description of how Maxwell−Stefan diffusivities in ternary systems follow from the Onsager coefficients Λ_{ij}. We also provide values for the self- and Maxwell−Stefan diffusivities of the investigated systems. This material is available free of charge via the Internet at http://pubs.acs.org.

■ AUTHOR INFORMATION

Corresponding Author
*E-mail: andre.bardow@ltt.rwth-aachen.de.

■ ACKNOWLEDGMENT

This work was performed as part of the Cluster of Excellence "Tailor-Made Fuels from Biomass", which is funded by the Excellence Initiative by the German federal and state governments to promote science and research at German universities.

■ REFERENCES

(1) Remsing, R. C.; Swatloski, R. P.; Rogers, R. D.; Moyna, G. *Chem. Commun.* **2006**, *12*, 1271–1273.
(2) Wasserscheid, P.; Welton, T. *Ionic Liquids in Synthesis*; Wiley-VCH: Weinheim, 2008.
(3) Zhang, Y.; Sun, C. Z.; Liang, J.; Shang, Z. C. *Chin. J. Chem.* **2010**, *28*, 2255–2259.
(4) Mallakpour, S.; Dinari, M. *J. Polym. Environ.* **2010**, *18*, 705–713.
(5) Jeihanipour, A.; Karimi, K.; Niklasson, C.; Taherzadeh, M. J. *Waste Manage.* **2010**, *30*, 2504–2509.
(6) Huddleston, J. G.; Willauer, H. D.; Swatloski, R. P.; Visser, A. E.; Rogers, R. D. *Chem. Commun.* **1998**, *16*, 1765–1766.
(7) Swatloski, R. P.; Spear, S. K.; Holbrey, J. D.; Rogers, R. D. *J. Am. Chem. Soc.* **2002**, *124*, 4974–4975.
(8) Youngs, T. G. A.; Hardacre, C.; Holbrey, J. D. *J. Phys. Chem.* **2007**, *111*, 13765–13774.
(9) Porter, A. R.; Liem, S. Y.; Popelier, P. L. A. *Phys. Chem. Chem. Phys.* **2008**, *10*, 4240–4248.
(10) Lovell, C. S.; Walker, A.; Damion, R. A.; Radhi, A.; Tanner, S. F.; Budtova, T.; Ries, M. E. *Biomacromolecules* **2010**, *11*, 2927–2935.
(11) Iacob, C.; Sangoro, J. R.; Papadopoulos, P.; Schubert, T.; Naumov, S.; Valiullin, R.; Karger, J.; Kremer, F. *Phys. Chem. Chem. Phys.* **2010**, *12*, 13798–13803.
(12) Bara, J. E.; Carlisle, T. K.; Gabriel, C. J.; Camper, D.; Finotello, A.; Gin, D. L.; Noble, R. D. *Ind. Eng. Chem. Res.* **2009**, *48*, 2793–2751.
(13) Borodin, O.; Smith, D. *J. Phys. Chem. B* **2006**, *110*, 11481–11490.
(14) Liu, Z. P.; Chen, T.; Bell, A.; Smit, B. *J. Phys. Chem. B* **2010**, *114*, 4572–4582.
(15) Liu, X.; Vlugt, T. J. H.; Bardow, A. *Fluid Phase Equilib.* **2011**, *301*, 110–117.
(16) Méndez-Morales, T.; Carrete, J.; Cabeza, O.; Gallego, L.; Varela, L. *J. Phys. Chem. B* **2011**, *115*, 6995–7008.
(17) Sarraute, S.; Costa Gomes, M. F.; Padua, A. A. H. *J. Chem. Eng. Data* **2009**, *54*, 2389–2394.
(18) Su, W. C.; Chou, C. H.; Wong, D. S. H.; Li, M. H. *J. Solution Chem.* **2007**, *252*, 74–78.
(19) Wong, C. L.; Soriano, A. N.; Li, M. H. *Fluid Phase Equilib.* **2008**, *271*, 43–52.
(20) Heintz, A.; Lehmann, J.; Schmidt, E.; Wandschneider, A. *J. Solution Chem.* **2009**, *38*, 1079–1083.
(21) Nieto de Castro, C. A.; Langa, E.; Morais, A. L.; Matos Lopes, M. L.; Lourenco, M. J. V.; Santos, F. J. V.; Santos, M. S. C. S.; Canongia Lopes, J. N.; Veiga, H. I. M.; Macatrao, M.; Esperanca, J. M. S. S.; Marques, C. S.; Rebelo, L. P. N.; Afonso, C. A. M. *Fluid Phase Equilib.* **2010**, *294*, 157–179.
(22) Heintz, A.; Ludwig, R.; Schmidt, E. *Phys. Chem. Chem. Phys.* **2011**, *13*, 3268–3273.
(23) Richter, J.; Leuchter, A.; Grosser, N. *J. Mol. Liq.* **2003**, *103−104*, 359–370.
(24) Liu, X.; Bardow, A.; Vlugt, T. J. H. *Ind. Eng. Chem. Res.* **2011**, *50*, 4776–4782.
(25) Frenkel, D.; Smit, B. *Understanding molecular simulation: From algorithms to applications*; Academic Press: San Diego, 2002.
(26) Dubbeldam, D.; Ford, D. C.; Ellis, D. E.; Snurr, R. Q. *Mol. Simul.* **2009**, *35*, 1084–1097.
(27) Krishna, R.; van Baten, J. M. *Ind. Eng. Chem. Res.* **2005**, *44*, 6939–6947.
(28) Wu, Y.; Tepper, H. L.; Voth, G. A. *J. Chem. Phys.* **2006**, *124*, 24503.
(29) Allen, M. P.; Tildesley, D. J. *Computer Simulation of Liquids*; Oxford University Press: New York, 1987.
(30) Chalaris, M.; Marinakis, S.; Dellis, D. *Fluid Phase Equilib.* **2008**, *267*, 47–60.
(31) Chen, T.; Chidambaram, M.; Liu, Z. P.; Smit, B.; Bell, A. T. *J. Phys. Chem. B* **2010**, *114*, 5790–5794.
(32) Taylor, R.; Kooijman, H. A. *Chem. Eng. Commun.* **1991**, *102*, 87–106.
(33) Krishna, R.; Wesselingh, J. A. *Chem. Eng. Sci.* **1997**, *52*, 861–911.
(34) Taylor, R.; Krishna, R. *Multicomponent mass transfer*; Wiley: New York, 1993.
(35) Poling, B. E.; Prausnitz, J. M.; O'Connell, J. P. *The properties of gases and liquids*; McGraw-Hill: New York, 2001.
(36) Bardow, A.; Kriesten, M. A.; Voda, E.; Casanova, F.; Blümich, B.; Marquardt, W. *Fluid Phase Equilib.* **2009**, *278*, 27–35.
(37) Wesselingh, J. A.; Krishna, R. *Elements of mass transfer*; Ellis Hoewood: Chichester, 1990.
(38) Kooijman, H. A.; Taylor, R. *Ind. Eng. Chem. Res.* **1991**, *30*, 1217–1222.
(39) Rehfeldt, S.; Stichlmair, J. *Fluid Phase Equilib.* **2007**, *256*, 99–104.
(40) Rehfeldt, S.; Stichlmair, J. *Fluid Phase Equilib.* **2010**, *290*, 1–14.
(41) Newman, J. S. *Electrochemical systems*; Prentice Hall, Inc.: Upper Saddle River, NJ, 1991.
(42) Feng, S. L.; Voth, G. A. *Fluid Phase Equilib.* **2010**, *294*, 148–156.
(43) Bordallo, H. N.; Herwig, K. W.; Luther, B. M.; Levinger, N. E. *J. Chem. Phys.* **2004**, *121*, 12457.
(44) Nieto-Draghi, C.; Avalos, J. B.; Rousseau, B. *J. Chem. Phys.* **2003**, *119*, 4782–4789.
(45) Soper, A. K.; Luzar, A. *J. Phys. Chem.* **1996**, *100*, 1357–1367.
(46) Miyanaga, S.; Tamura, K.; Murakami, S. *J. Therm. Anal.* **1992**, *38*, 1767–2589.

(47) Soper, A. K.; Luzar, A. *J. Chem. Phys.* **1992**, *97*, 1320–1331.
(48) Luzar, A.; Chandler, D. *J. Chem. Phys.* **1993**, *98*, 8160–8173.
(49) Vaisman, I. I.; Berkowitz, M. L. *J. Am. Chem. Soc.* **1992**, *114*, 7889–7896.
(50) Remsing, R. C.; Liu, Z. W.; Sergeyev, I.; Moyna, G. *J. Phys. Chem. B* **2008**, *112*, 7363–7369.
(51) Domanska, U.; Bogel-Lukasik, E.; Bogel-Lukasik, R. *Chem.—Eur. J.* **2003**, *9*, 3033–3041.
(52) Zhao, W.; Leroy, F.; Heggen, B.; Zahn, S.; Kirchner, B.; Balasubramanian, S.; Müller-Plathe, F. *J. Am. Chem. Soc.* **2009**, *131*, 15825–15833.
(53) Zhang, Y. T.; Du, X. H.; Qian, H. B.; Chem, E. Y. X. *J. Am. Chem. Soc.* **2010**, *24*, 2410–2417.
(54) Shekaari, H.; Mousavi, S. S. *J. Chem. Eng. Data* **2009**, *54*, 823–829.
(55) Fredlake, C. P.; Crosthwaite, J. M.; Hert, D. G.; Aki, S. N. V. J.; Brennecke, J. F. *J. Chem. Eng. Data* **2004**, *49*, 954–964.
(56) Gan, Q.; Rooney, D.; Xue, M. L.; Thompson, G.; Zou, Y. R. *J. Mol. Struct.* **2006**, *280*, 948–956.
(57) Nikam, P. S.; Jadhav, M. C.; Hasan, M. *J. Chem. Eng. Data* **1996**, *41*, 1028–1031.
(58) Holz, M.; Heil, S.; Sacco, A. *Phys. Chem. Chem. Phys.* **2000**, *2*, 4740–4742.
(59) Kell, G. S. *J. Chem. Phys.* **1967**, *12*, 66–69.
(60) Kell, G. S. *J. Chem. Eng. Data* **1975**, *20*, 97–105.
(61) Pruppacher, H. R. *J. Chem. Phys.* **1972**, *56*, 101–107.
(62) Fanninm, A. A.; Floreani, D. A.; King, L. A.; Landers, J. S.; Piersma, B. J.; Stch, D. J.; Vaughn, R. L.; Wilkes, J. S.; Williams, J. L. *J. Phys. Chem.* **1984**, *88*, 2614–2621.
(63) Dong, L.; Zheng, D. X.; Wei, Z.; Wu, X. H. *Int. J. Thermophys.* **2009**, *30*, 1480–1490.
(64) Shukla, M.; Srivastava, N.; Saha, S. *J. Mol. Struct.* **2010**, *975*, 349–356.